Bautista, Godofredo; Kakko, Joona Pekko; Dhaka, Veer; Zang, Xiaorun; Karvonen, Lasse; Jiang, Hua; Kauppinen, Esko; Lipsanen, Harri; Kauranen, Martti

Nonlinear microscopy using cylindrical vector beams

Published in:
Optics Express

DOI:
10.1364/OE.25.012463

Published: 29/05/2017

Document Version
Publisher's PDF, also known as Version of record

Research Article | Vol. 25, No. 11 | 29 May 2017 | OPTICS EXPRESS 12463
Optics EXPRESS

Nonlinear microscopy using cylindrical vector beams: applications to three-dimensional imaging of nanostructures

GODOFREDO BAUTISTA,[1,*] JOONA-PEKKO KAKKO,[2] VEER DHAKA,[2] XIAORUN ZANG,[1] LASSE KARVONEN,[2] HUA JIANG,[3] ESKO KAUPPINEN,[3] HARRI LIPSANEN,[2] AND MARTTI KAURANEN[1]

[1]*Laboratory of Photonics, Tampere University of Technology, P. O. Box 692, FI-33101 Tampere, Finland*
[2]*Department of Electronics and Nanoengineering, Aalto University, P.O. Box 13500, FI-00076 Aalto, Finland*
[3]*Department of Applied Physics and Nanomicroscopy Center, Aalto University, P.O. Box 15100, FI-00076 Aalto, Finland*
**godofredo.bautista@tut.fi*

Abstract: The three-dimensional (3D) optical fields that arise from the focusing of cylindrical vector beams (CVB) with radial and azimuthal polarizations provide new sources of contrast for optical microscopy of nano-objects. So far, these demonstrations have been restricted to two-dimensional transversal scanning, i.e., along the focal plane of interest, or use of point-like objects, i.e., single molecules and nanoparticles. Here, we demonstrate the first application of CVBs for 3D imaging of 3D nano-objects. This technique is done by acquiring 3D image scans of the second-harmonic generation signal from vertically-aligned semiconductor nanowires, whose second-order response is primarily driven by the longitudinal electric field, i.e., the field component along the nanowire axis. Our technique provides a new way to study individual nano-objects in three dimensions through the unique combination of nonlinear microscopy and CVBs.

OCIS codes: (170.6900) Three-dimensional microscopy; (180.4315) Nonlinear microscopy; (190.4180) Multiphoton processes; (260.5430) Polarization; (310.6628) Subwavelength structures, nanostructures.

References and links

1. Q. Zhan, "Cylindrical vector beams: From mathematical concepts to applications," Adv. Opt. Photonics **1**(1), 1–57 (2009).
2. T. G. Brown, "Chapter 2 - Unconventional polarization states: beam propagation, focusing, and imaging," Prog. Opt. **56**, 81–129 (2011).
3. T. Züchner, A. V. Failla, and A. J. Meixner, "Light microscopy with doughnut modes: a concept to detect, characterize, and manipulate individual nanoobjects," Angew. Chem. Int. Ed. Engl. **50**(23), 5274–5293 (2011).
4. R. Dorn, S. Quabis, and G. Leuchs, "Sharper focus for a radially polarized light beam," Phys. Rev. Lett. **91**(23), 233901 (2003).
5. S. Quabis, R. Dorn, M. Eberler, O. Glöckl, and G. Leuchs, "Focusing light to a tighter spot," Opt. Commun. **179**(1-6), 1–7 (2000).
6. K. Youngworth and T. Brown, "Focusing of high numerical aperture cylindrical-vector beams," Opt. Express **7**(2), 77–87 (2000).
7. A. V. Nesterov and V. G. Niziev, "Propagation features of beams with axially symmetric polarization," J. Opt. B Quantum Semiclassical Opt. **3**(2), S215–S219 (2001).
8. C. J. R. Sheppard and A. Choudhury, "Annular pupils, radial polarization, and superresolution," Appl. Opt. **43**(22), 4322–4327 (2004).
9. L. Novotny, M. R. Beversluis, K. S. Youngworth, and T. G. Brown, "Longitudinal field modes probed by single molecules," Phys. Rev. Lett. **86**(23), 5251–5254 (2001).
10. M. Fleischer, C. Stanciu, F. Stade, J. Stadler, K. Braun, A. Heeren, M. Häffner, D. P. Kern, and A. J. Meixner, "Three-dimensional optical antennas: Nanocones in an apertureless scanning near-field microscope," Appl. Phys. Lett. **93**(11), 111114 (2008).
11. A. V. Failla, H. Qian, H. Qian, A. Hartschuh, and A. J. Meixner, "Orientational imaging of subwavelength Au particles with higher order laser modes," Nano Lett. **6**(7), 1374–1378 (2006).

#291656 https://doi.org/10.1364/OE.25.012463
Journal © 2017 Received 28 Mar 2017; revised 13 May 2017; accepted 14 May 2017; published 18 May 2017

Optics EXPRESS

12. H. Ishitobi, I. Nakamura, N. Hayazawa, Z. Sekkat, and S. Kawata, "Orientational imaging of single molecules by using azimuthal and radial polarizations," J. Phys. Chem. B **114**(8), 2565–2571 (2010).
13. Y. Saito, M. Kobayashi, D. Hiraga, K. Fujita, S. Kawano, N. I. Smith, Y. Inouye, and S. Kawata, "Z-polarization sensitive detection in micro-Raman spectroscopy by radially polarized incident light," J. Raman Spectrosc. **39**(11), 1643–1648 (2008).
14. M. Kasperczyk, S. Person, D. Ananias, L. D. Carlos, and L. Novotny, "Excitation of magnetic dipole transitions at optical frequencies," Phys. Rev. Lett. **114**(16), 163903 (2015).
15. G. Bautista and M. Kauranen, "Vector-field nonlinear microscopy of nanostructures," ACS Photonics **3**(8), 1351–1370 (2016).
16. K. Yoshiki, M. Hashimoto, and T. Araki, "Second-harmonic-generation microscopy using excitation beam with controlled polarization pattern to determine three-dimensional molecular orientation," Jpn. J. Appl. Phys. **44**(34), L1066–L1068 (2005).
17. E. Y. S. Yew and C. J. R. Sheppard, "Second harmonic generation polarization microscopy with tightly focused linearly and radially polarized beams," Opt. Commun. **275**(2), 453–457 (2007).
18. G. Bautista, M. J. Huttunen, J. Mäkitalo, J. M. Kontio, J. Simonen, and M. Kauranen, "Second-harmonic generation imaging of metal nano-objects with cylindrical vector beams," Nano Lett. **12**(6), 3207–3212 (2012).
19. M. J. Huttunen, K. Lindfors, D. Andriano, J. Mäkitalo, G. Bautista, M. Lippitz, and M. Kauranen, "Three-dimensional winged nanocone optical antennas," Opt. Lett. **39**(12), 3686–3689 (2014).
20. G. Bautista, M. J. Huttunen, J. M. Kontio, J. Simonen, and M. Kauranen, "Third- and second-harmonic generation microscopy of individual metal nanocones using cylindrical vector beams," Opt. Express **21**(19), 21918–21923 (2013).
21. G. Bautista, J. Mäkitalo, Y. Chen, V. Dhaka, M. Grasso, L. Karvonen, H. Jiang, M. J. Huttunen, T. Huhtio, H. Lipsanen, and M. Kauranen, "Second-harmonic generation imaging of semiconductor nanowires with focused vector beams," Nano Lett. **15**(3), 1564–1569 (2015).
22. L. Turquet, J.-P. Kakko, X. Zang, L. Naskali, L. Karvonen, H. Jiang, T. Huhtio, E. Kauppinen, H. Lipsanen, M. Kauranen, and G. Bautista, "Tailorable second-harmonic generation from an individual nanowire using spatially phase-shaped beams," Laser Photonics Rev. **11**(1), 1600175 (2017).
23. F. Lu, W. Zheng, and Z. Huang, "Coherent anti-Stokes Raman scattering microscopy using tightly focused radially polarized light," Opt. Lett. **34**(12), 1870–1872 (2009).
24. X. Li, T.-H. Lan, C.-H. Tien, and M. Gu, "Three-dimensional orientation-unlimited polarization encryption by a single optically configured vectorial beam," Nat. Commun. **3**, 998 (2012).
25. R. Sanatinia, S. Anand, and M. Swillo, "Modal engineering of second-harmonic generation in single GaP nanopillars," Nano Lett. **14**(9), 5376–5381 (2014).
26. A. Casadei, E. F. Pecora, J. Trevino, C. Forestiere, D. Rüffer, E. Russo-Averchi, F. Matteini, G. Tutuncuoglu, M. Heiss, A. Fontcuberta i Morral, and L. Dal Negro, "Photonic-plasmonic coupling of GaAs single nanowires to optical nanoantennas," Nano Lett. **14**(5), 2271–2278 (2014).
27. M. Timofeeva, A. Bouravleuv, G. Cirlin, I. Shtrom, I. Soshnikov, M. Reig Escalé, A. Sergeyev, and R. Grange, "Polar second-harmonic imaging to resolve pure and mixed crystal phases along GaAs nanowires," Nano Lett. **16**(10), 6290–6297 (2016).

1. Introduction

Cylindrical vector beams (CVB), e.g., radially- and azimuthally-polarized beams, and their applications in optical microscopy are subjects of growing interest [1–3]. This is mainly due to the unique properties of CVBs when strongly focused by a microscope objective [4–8]. For example, the focusing of a radially-polarized beam creates a unique three-dimensional (3D) focal-field distribution that exhibits radially-polarized transversal electric components at the focal plane and non-negligible longitudinal components along the axis of beam propagation. In contrast, the focusing of an azimuthally-polarized beam creates a focal-field distribution that exhibits purely azimuthally-polarized transversal electric fields at the focal plane. For years, the complementary focusing properties of CVBs have been used to increase the contrast and sensitivity of linear [9–14] and nonlinear [15–24] microscopy techniques. So far, the previous microscopy demonstrations have been restricted to two-dimensional (2D) image scanning, i.e., along the focal plane of interest, or the use of point-like objects, i.e., single molecules and nanoparticles. In this work, we demonstrate the first use of CVBs for 3D nonlinear imaging of 3D nanostructures.

2. Materials and methods

Our technique is based on a point-scanning second-harmonic generation (SHG) microscope [Fig. 1(a)]. Previously, we have used this microscopy configuration to study the nonlinear response of individual metal [15,18–20] and semiconductor nano-objects [21,22]. A

Optics EXPRESS

femtosecond laser (1060 nm, 140 or 200 fs, 80 MHz) is used as the excitation source. The output of this laser is polarization- and spatially-cleaned and then directed to the microscope objective (numerical aperture (NA) of 0.8). The SHG signals from the samples are collected by the same objective. The signals are directed to a photomultiplier tube that is equipped with appropriate optical filters. To create a scanning image, the sample is mounted on a computer-controlled 3D piezo-scanning system. The samples are scanned at different focal plane positions and orientations, e.g., at *xy* transversal planes or longitudinal planes where one of the acquisition directions is set along the *z*-axis. A pixel dwell time of 100 or 50 ms is used. A half-wave plate is used to create the desired linear polarization orientation. A polarization mode converter (Arcoptix S.A.) and a spatial filter are used to create radial and azimuthal CVBs. For comparison, the same regions of interest in the sample are imaged. To prevent sample damage during the nonlinear experiments, an average input power of 1 mW is used. For image plotting, Matlab and ImageJ were used.

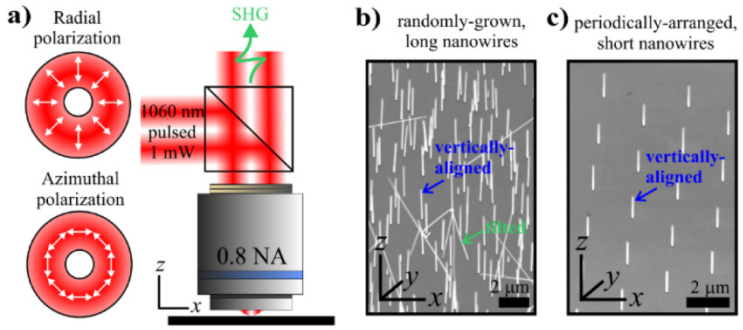

Fig. 1. (a) Scheme of the nonlinear microscope that uses radial and azimuthal CVB excitation. (b) Scanning electron micrographs of vertically-aligned GaAs nanowires on GaAs substrate with random (left) and periodic (right) arrangements.

Two different semiconductor nanowire samples consisting of pristine vertically-aligned GaAs nanowires on GaAs substrates are investigated in our 3D imaging demonstrations. We previously found that the SHG signals from these vertically-oriented nanowires are primarily driven by the longitudinal electric fields at the beam focus [21,22]. For the first application, we used GaAs nanowires that were randomly grown [similar to Fig. 1(b)]. As shown, the resulting samples contain nanowires with varying lengths and orientations with respect to the substrate normal. Based on previous structural investigations, the nanowires exhibit a length of 10 μm and a diameter of 40 nm. The details of the nanowire fabrication and related structural characterization are found in our previous work [21]. For the second application, we used GaAs nanowires that are periodically arranged and strictly vertically oriented [similar to Fig. 1(c)]. According to previous investigations, the nanowires exhibit a length of 1 μm, and a diameter of 40 nm. The details of the nanowire fabrication and structural characterization are similar to the samples used in our previous study [22].

3. Results and discussion

First, we demonstrate the optical sectioning capability of the SHG microscopy technique with CVBs using the nanowire samples in Fig. 1(b). Shown in Fig. 2(a) are the depth-resolved SHG intensity maps acquired from the long nanowire samples using linearly-, radially-, and azimuthally-polarized beams. Here, the (air-GaAs substrate) interface is located at $z = 0$ plane. In this 3D microscopy data, the advantages of CVBs for imaging nano-objects in three dimensions are obvious. For comparison, we also show the predicted intensity patterns of the longitudinal electric fields (E_z) at the beam focus for different polarizations using the Debye method [Fig. 2(b)].

Optics EXPRESS

We first acquired the SHG images of these nanowires using linear polarizations [Fig. 2(a) (1st and 2nd rows from top)]. The SHG intensity maps of the vertically-aligned nanowires exhibit two-lobed patterns that rotate with the orientation of the linearly-polarized input [21,22]. These patterns are similar to the spatial distribution of the longitudinal electric fields of the excitation beams [Fig. 2(b)]. The additional strong SHG signals arise from wires that are almost horizontal and aligned close to the incident polarization.

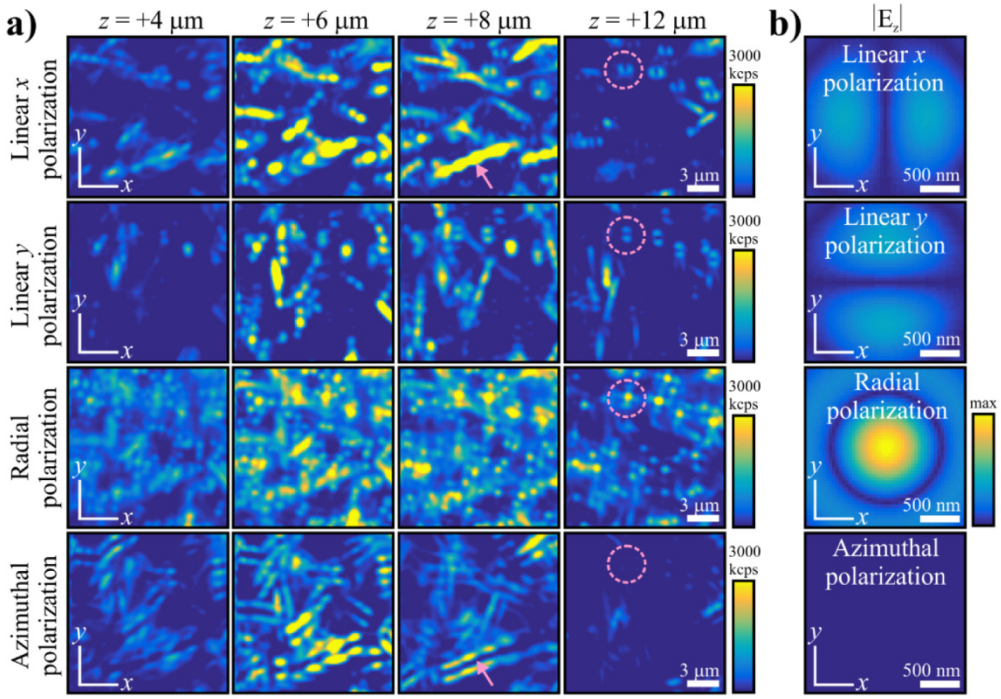

Fig. 2. (a) Experimental SHG intensity maps of vertically-aligned GaAs nanowires randomly-grown on GaAs substrate. The maps were taken at different z-positions (see columns) above the substrate (z = 0). The maps were acquired for linear x (see Visualization 1), linear y (see Visualization 2), radial (see Visualization 3) and azimuthal (see Visualization 4) polarizations (see rows). The pixel dwell time is 100 ms. Representative intensity patterns from an individual nanowire are marked (pink circles or arrows). (b) Predicted intensity patterns of the longitudinal electric field (E_z) at the beam focus, i.e., at the transverse mirror plane, using the same experiment settings.

Using a radially-polarized beam, the vertically-aligned nanowires exhibit point-spread-like SHG intensity distributions [Fig. 2(a) (3rd row from top)], mimicking the spatial distribution of the longitudinal electric fields of the excitation beam [Fig. 2(b)]. The signals from the vertically-aligned nanowires are also generally greater than the signals acquired with the linearly-polarized beams confirming efficient excitation of these nanowires with radial polarization. These results are consistent with previous works on these nanowires [21,22]. We assign variations in the SHG intensities to possible variations in the lengths of the nanowires.

For azimuthally-polarized excitation, the SHG intensities from the same vertically-aligned nanowires remain very small [Fig. 2 (bottom row)] due to the absence of a longitudinal electric field at the focus for this case [Fig. 2(b)]. We assign the residual SHG signals from the asymmetric excitation of nanowires that have tilted or near-horizontal orientations and excited by the purely transversal electric fields of the impinging excitation beam. Due to the rotational symmetry of the azimuthally-polarized focus, we see double images of the tilted nanowires as expected [1–3]. Interestingly, the use of an azimuthally-polarized beam revealed that the fabrication process indeed resulted in some nanowires with different tilted

Optics EXPRESS

orientations. This imaging capability significantly reduces the number of sequential measurements that are traditionally done with linearly-polarized beams [Fig. 2(a) (1st and 2nd rows from top)]. Finally, the SHG intensity patterns of the tilted nanowires revealed periodic intensity variations along the long axis of some nanowires using azimuthally and linearly-polarized beams [marked by arrows in Fig. 2(a)]. The origin of these variations are unknown at this time but could be due to the diameter-dependent optical modes that propagate along the nanowire [25]. In the future, it would be interesting to study these effects in individual nanowires in three dimensions using this imaging technique.

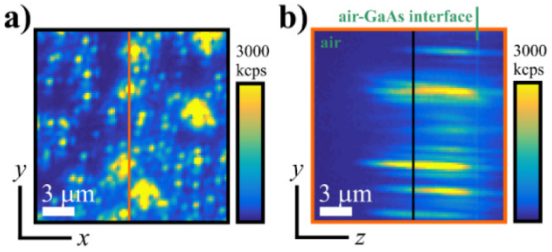

Fig. 3. Experimental SHG 3D intensity maps of vertically-aligned GaAs nanowires randomly-grown on GaAs substrate. The maps were taken at the (a) transversal, i.e., *xy*, plane that is 6 μm above the substrate and (b) longitudinal planes, i.e., *zy*, using a radially-polarized beam. The corresponding focal planes are color-coded (black and orange solid lines and squares). The pixel dwell time is 100 ms. In (b), the location of the air-GaAs substrate interface is marked (green solid line).

Using the radially-polarized beam, we again acquired the SHG image of the same vertically-aligned nanowires (in a different region). As expected, the SHG intensity maps of the nanowires exhibit varied point-spread-like intensity distributions when viewed in the transversal plane [Fig. 3(a)]. Most importantly, a single longitudinal, i.e. *zy*, SHG scan at a fixed transverse position (in *x*) clearly reveals several needle-like intensity distributions of varying spatial extent along the *z*-axis [Fig. 3(b)]. We can associate these intensity distributions to nanowires of different lengths. In addition, any deviations from the resulting needle-like intensity distributions in the longitudinal scans could possibly indicate the presence of defects in the nanowires (e.g., twinning defects, voids, contaminants). We note that such features are obscured in a single transversal scan even with a radially-polarized beam [Fig. 3(a)]. The location of the air-GaAs interface was determined by taking the *z*-dependent SHG signal from the substrate, i.e., from regions in the samples without nanowires. Overall, these results further attest the potential of 3D nonlinear microscopy with CVBs.

Finally, we note that our previous imaging demonstrations (Figs. 2 and 3) are still possibly plagued by crosstalk among the nanowires thereby preventing one to study in detail an individual nanowire. To circumvent this issue, we further demonstrate the 3D imaging capability of CVBs using well-separated and vertically-oriented nanowires [Fig. 1(c)]. The transversal scanning planes reveal the presence of four nanowires in the region of interest which are only excited by the longitudinal electric fields of a radially-polarized beam [Figs. 4(a) and 4(b)]. We next focus on one of the nanowires (e.g., wire on the left) and perform a longitudinal scan at a fixed position in the *x*-axis. The longitudinal scans again reveal the needle-like intensity distribution of the nanowire with radially-polarized excitation. The line cuts further reveal that the nanowire under a radially-polarized beam exhibits a maximum SHG signal that is about 10 times the signal from that of the GaAs-air interface [Fig. 4(c)]. This is consistent with previous findings that SHG from GaAs nanowires is indeed more efficient than from their bulk counterparts [21,22,26,27]. The line cut from the nanowire under a radially-polarized beam also reveals a maximum that is around 1 μm from the peak of the line cuts derived from the substrate using both CVBs. The position of this peak indicates the optimal positions along the *z*-axis where a nanowire can be efficiently excited. A slight

Optics EXPRESS

asymmetry is also seen in the line cut derived from the nanowire. This is most likely from coupling between the signals from the nanowire and the nearby substrate. This method can therefore be useful in investigating the effects of surface passivation on the nonlinear emission of such nanostructures. Such imaging experiments could be very tedious to do in individual nano-objects using traditional optical microscopy techniques.

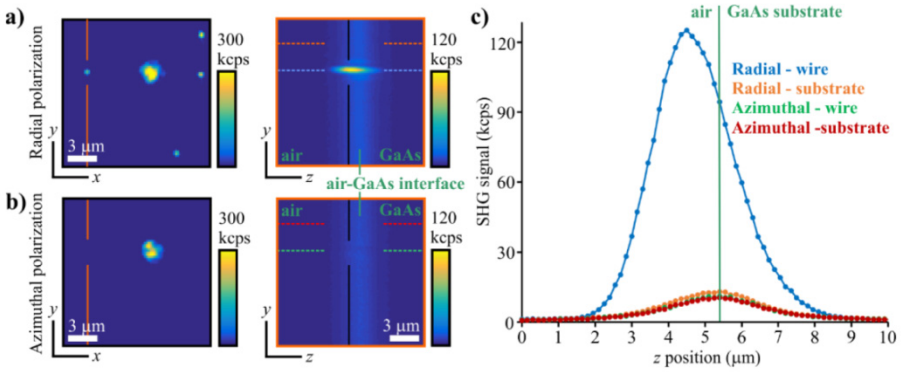

Fig. 4. Experimental SHG 3D intensity maps of four vertically-aligned GaAs nanowires periodically-arranged on GaAs substrate. The maps were taken at the transversal plane (at 1 μm above the substrate) and the longitudinal plane using (a) radially and (b) azimuthally-polarized beams. The corresponding focal planes are color-coded (black and orange solid lines and squares). The pixel dwell time is 50 ms. The location of the air-GaAs interface is shown (green solid line). (c) SHG line cuts extracted from the longitudinal scans from a single nanowire in (a,b). The data from the wire and substrate for different CVBs are color-coded [dashed lines in (a,b)]. The location of the air-GaAs interface is shown (green solid line).

We acknowledge that the CVBs combined with the 3D nonlinear imaging technique can unambiguously recognize vertically-aligned semiconductor nanowires. So far, we do not yet have the capability to determine the 3D tilt or orientation of these semiconductor nanowires in space. This can be done by studying the SHG from semiconductor nanowires with known 3D tilts. Perhaps, what is even important in the future is the 3D noninvasive all-optical detection of the growth orientation and crystal structure (e.g., zinc-blende or wurtzite) of these semiconductor nanowires. Although SHG imaging with linear polarizations was used recently to identify the crystal orientation of GaAs nanowires [27], the crystal structure detection of vertically-aligned nanowires using SHG imaging with CVBs remains unexplored.

4. Conclusions

We have demonstrated the first use of radially- and azimuthally-polarized beams for 3D imaging of real nano-objects. The technique is based on 3D acquisition of SHG signals from vertically-aligned semiconductor nanowires, whose second-order response is primarily driven by the field component along the nanowire axis. The technique is opening new ways to investigate individual nano-objects in three dimensions through the unique combination of nonlinear microscopy and CVBs.

Funding

Academy of Finland (267847, 287651, 284529); Investment funding of the Tampere University of Technology (84010); TEKES FiDiPro NP-Nano project.

Acknowledgments

Nanowire fabrication was performed at the Micronova Nanofabrication Centre of Aalto University. This work made use of the Aalto University Nanomicroscopy Center (Aalto-NMC) premises. This work was performed in the context of the European COST Action MP1302 Nanospectroscopy.